Effects of Collision Dynamics on Interaction Study via Femtoscopy

SOPHIA U

SOPHIA HADRON PHYSICS GROUP

arXiv:2410.01204 [hep-ph]

Kenshi Kuroki (Sophia University, JP)
k-kuroki-e23@eagle.sophia.ac.jp

In collaboration with

Tetsufumi Hirano (Sophia University, JP)

Basics of Femtoscopy

- Correlation Function
- Koonin-Pratt Formula
- Current Situation

Hadron Correlations

Momentum correlations in **high-energy nuclear collisions**
→ Useful for studying **low-energy hadron interactions**

Correlation Function (CF) at Pair Rest Frame ($\boldsymbol{P} = 0$)

$$C(\boldsymbol{q}) \coloneqq \frac{N_{\mathrm{pair}}(\boldsymbol{p}_a, \boldsymbol{p}_b)}{N_a(\boldsymbol{p}_a)\, N_b(\boldsymbol{p}_b)}$$

Total momentum: $\boldsymbol{P} = \boldsymbol{p}_a + \boldsymbol{p}_b$
Relative momentum: $\boldsymbol{q} = \frac{m_b \boldsymbol{p}_a - m_a \boldsymbol{p}_b}{m_a + m_b}$
Two-particle momentum dist.: $N_{\mathrm{pair}}(\boldsymbol{p}_a, \boldsymbol{p}_b)$
One-particle momentum dist.: $N_a(\boldsymbol{p}_a)$

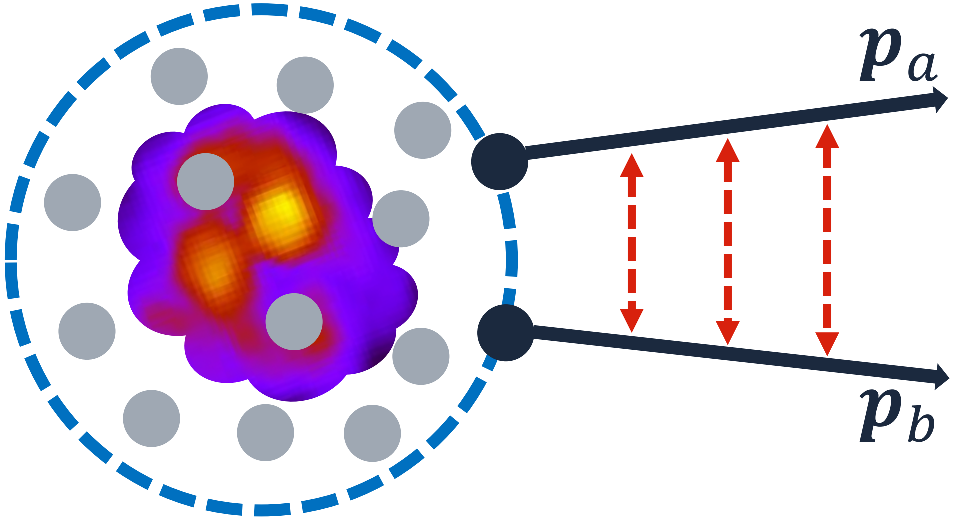

Hadron CF provides insights into

- **Space-time structure of the matter**
- **Final state hadron interactions**

Koonin-Pratt formula

S. E. Koonin, PLB **70**, 43 (1977); S. Pratt, PRL **53**, 1219 (1984)

Under several assumptions,

$$C(\boldsymbol{q}) = \int d^3r\ S(\boldsymbol{q};\boldsymbol{r})\ |\varphi(\boldsymbol{q};\boldsymbol{r})|^2$$

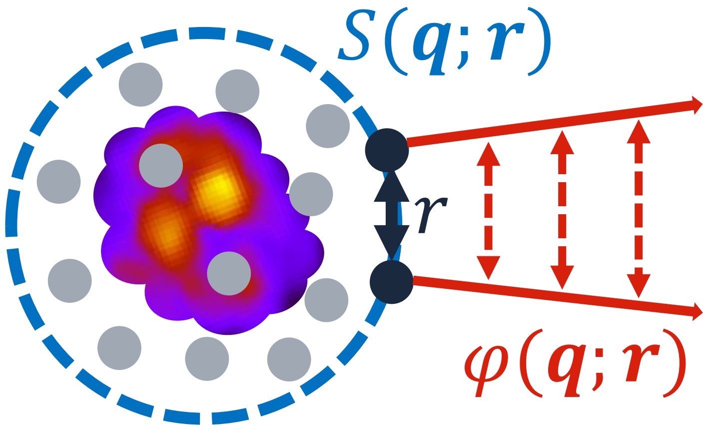

CF ⇐ **Source Func.** & **Relative WF**

From **experimental** correlation function

- **Input**: hadron interaction → **Output**: source function
- **Input**: source function → **Output**: hadron interaction

Wave Function with Final State Interaction

Focusing on low-q region with chaotic source and closed system assumptions

→ Steady-state Schrödinger eq. with central force

Partial-wave expansion

$$\varphi(\boldsymbol{q};\boldsymbol{r}) = \sum_{l=0}^{\infty}(2l+1)i^l\varphi_l(q;r)P_l(\cos\theta)$$

For each ${}^{2S+1}L_J$ channel,

$$\left[-\frac{1}{2\mu}\frac{d^2}{dr^2} + V(r) + \frac{1}{2\mu}\frac{l(l+1)}{r^2}\right]u_l(q;r) = \frac{q^2}{2\mu}u_l(q;r)$$

$$u_l := r\,\varphi_l$$

$$\mu = \frac{m_a m_b}{m_a + m_b}$$

Rewriting Koonin-Pratt Formula

For non-identical pair,

Spherical SF
$S(q;r)$

Only *s*-wave scattering

$$\varphi(\boldsymbol{q};\boldsymbol{r}) = \exp(i\boldsymbol{q}\cdot\boldsymbol{r}) - j_0(qr) + \varphi_0(q;r)$$

Plane-wave | **Plane-wave (*s*-wave)** | **WF (*s*-wave)**

$$C(\boldsymbol{q}) = \int d^3r\, S(\boldsymbol{q};\boldsymbol{r})\, |\varphi(\boldsymbol{q};\boldsymbol{r})|^2$$

$$= 1 + \int_0^\infty dr\, 4\pi r^2 S(q;r)\, \left[|\varphi_0(q;r)|^2 - |j_0(qr)|^2\right]$$

SF
with Jacobian

***s*-wave Change**
Increase/Decrease of WF by **FSI**

Interpretation of Correlation Function

$$C(q) = 1 + \int_0^\infty dr \; 4\pi r^2 S(q;r) \; [|\varphi_0(q;r)|^2 - |j_0(qr)|^2]$$

SF
with Jacobian

***s*-wave Change**
Increase/Decrease in WF by interaction

Deviation of $C(q)$ from 1 = **How much SF “picks up” WF change**

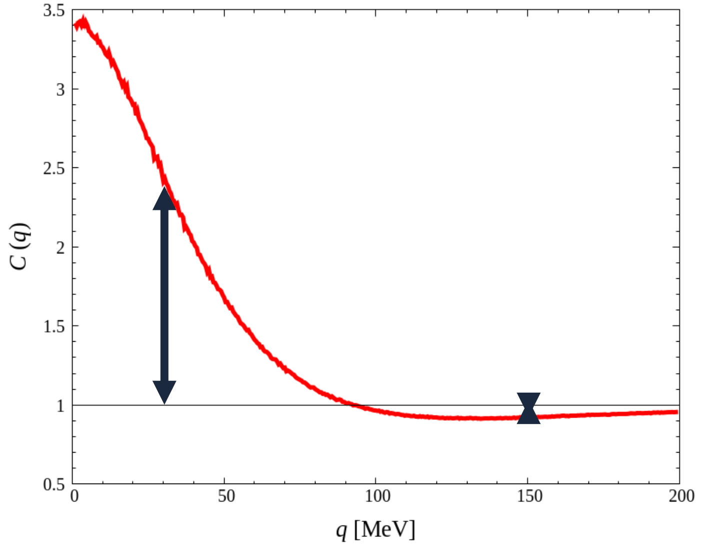

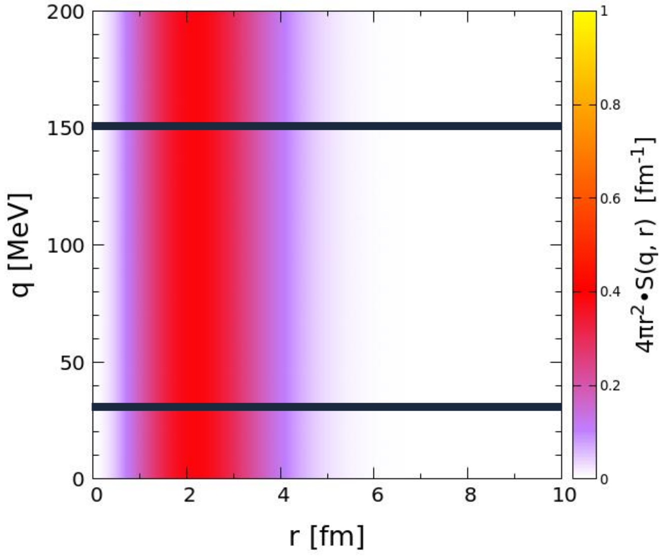

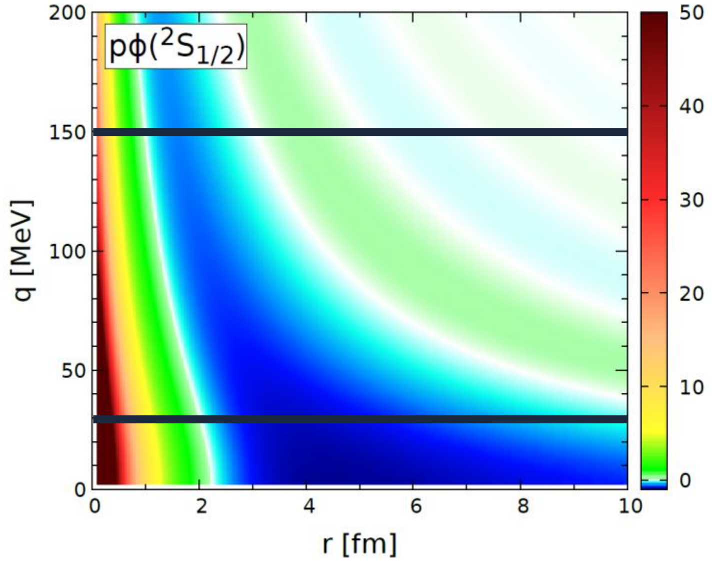

Hadron Interaction Study via Femtoscopy

Recent active studies have demonstrated its usefulness and powerfulness

L. Fabbietti *et al.*, Ann. Rev. Nucl. Part. Sci. **71**, 377 (2021)

→ Assuming **static Gaussian SF**

Actual SF should reflect the complex dynamics of nuclear collisions

A. Ohnishi, talk at RHIC-BES On-line seminar IV (2022)

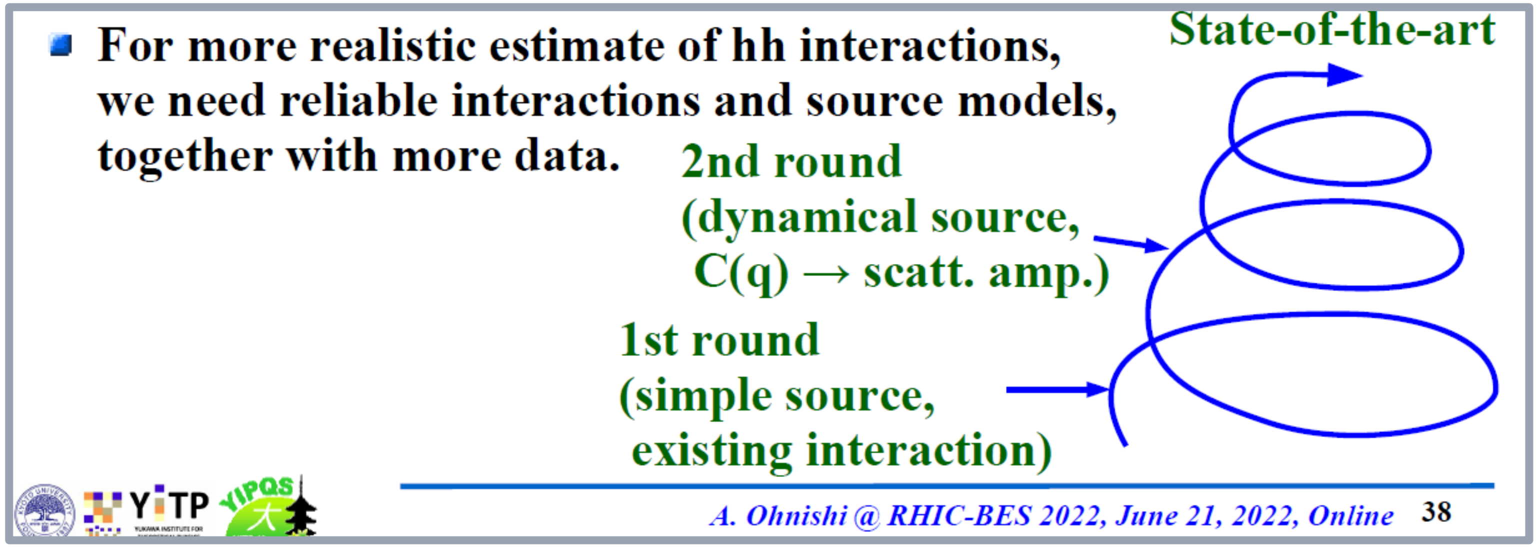

To explore less understood hadron interactions,

Femtoscopy using **dynamical models**

Spin-Averaged Correlation Function

WF in KP formula = Weighted average of WF in each $^{2S+1}L_J$ channel

$$|\varphi|^2 = \sum_{\text{states}(S,L,J)} \omega_{(S,L,J)} \left|\varphi^{(S,L,J)}\right|^2$$

$$\omega_{(S,L,J)} = \frac{2S+1}{(2s_a+1)(2s_b+1)} \frac{2J+1}{(2L+1)(2S+1)}$$

Koonin-Pratt formula

Spin-independent SF

$$C^{\text{tot}}(q) = \sum_{\text{states}(S,L,J)} \omega_{(S,L,J)}\, C^{(S,L,J)}(q)$$

⇒ Comparable with exp. CF

pϕ Femtoscopy using Dynamical Model

- Overview
- Interaction and Wave Function
- Source Function
- Correlation Function

Existing pϕ Femtoscopy 1

Experimental CF
ALICE, PRL **127**, 172301 (2021)

High-multiplicity (0–0.17%) **p+p collisions at** $\sqrt{s} = 13$ TeV

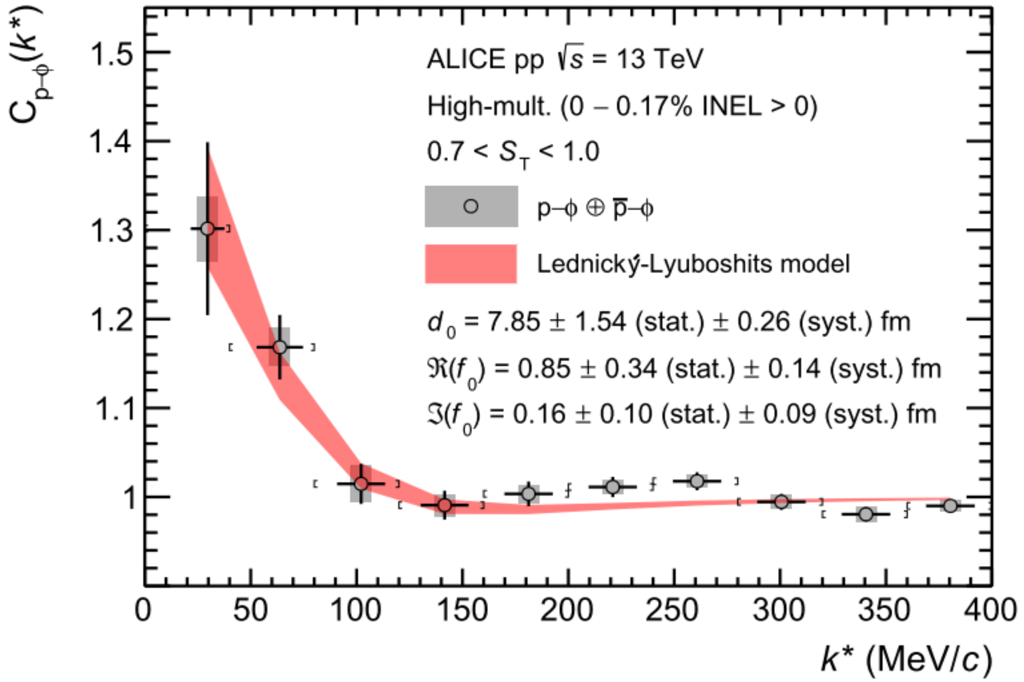

Lednický-Lyuboshits fit
R. Lednický and V. L. Lyuboshits, Yad. Fiz. **35**, 1316 (1981)

Gaussian source size: $r_0 = 1.08$ fm

Scattering length: $a_0 \cong -0.85 - 0.16i$ fm

Effective range: $r_{\mathrm{eff}} \cong 7.85$ fm

Attractive pϕ interaction **as a spin-average**

Existing pϕ Femtoscopy 2

Spin-channel-by-channel femtoscopy

E. Chizzali *et al.*, PLB **848**, 138358 (2023)

Gaussian source size: $r_0 = 1.08$ fm

$^4S_{3/2}$: HAL QCD potential Y. Lyu *et al.*, PRD 106, 074507 (2022)

$a_0^{(3/2)} \cong -1.43$ fm, $r_{\mathrm{eff}}^{(3/2)} \cong 2.36$ fm

Attraction without bound states

$^2S_{1/2}$: **Parametrized potential ← Constrain by experimental CF**

$a_0^{(1/2)} \cong 1.54 - i0.00$ fm, $r_{\mathrm{eff}}^{(1/2)} \cong 0.39 + i0.00$ fm

- **Strong attraction**
- **Small effects of channel-coupling**

Indication of a pϕ bound state

Overview of Present Study

This study: **pϕ Femtoscopy using SF from a dynamical model**

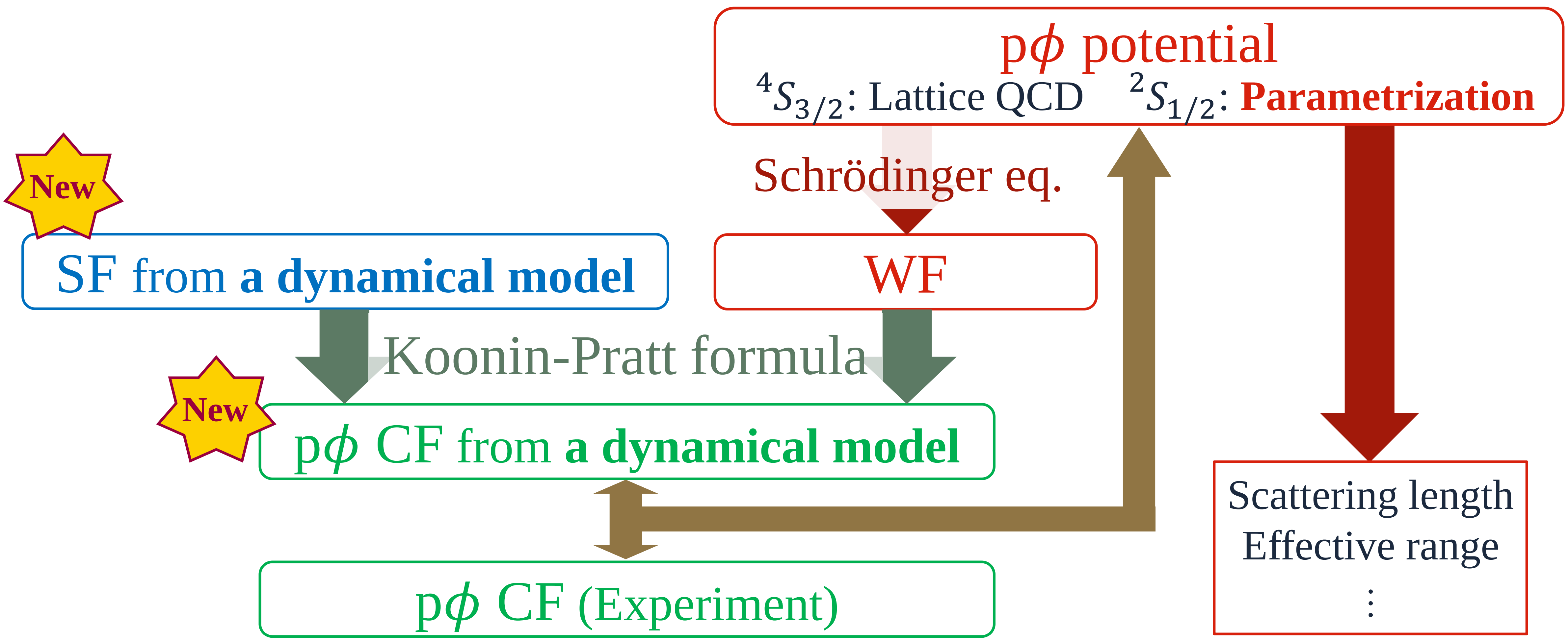

$^4S_{3/2}$ Channel

HAL QCD potential
Y. Lyu *et al.*, PRD **106**, 074507 (2022)

Lattice QCD at nearly physical point ($m_\pi = 146.4$ MeV)

$$V^{(3/2)}(r) = a_1 e^{-(r/b_1)^2} + a_2 e^{-(r/b_2)^2} + a_3 m_\pi^4 f(r;b_3) \frac{e^{-2m_\pi r}}{r^2}$$

Short-range attraction — TPE

Argonne-type form factor:

$$f(r;b_3) = \left[1 - e^{-(r/b_3)^2}\right]^2$$

Parameter	Fitted value
a_1 [MeV]	−371±27
b_1 [fm]	0.13±0.01
a_2 [MeV]	−119±39
b_2 [fm]	0.30±0.05
a_3 [fm^5]	−1.62±0.23
b_3 [fm]	0.63±0.04

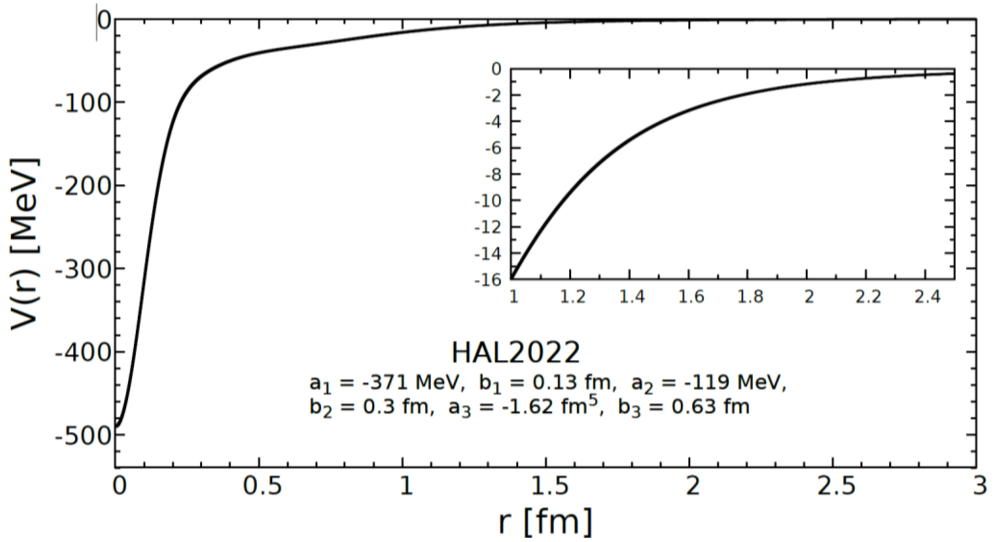

No bound state

WF change: $|\varphi_0|^2 - |j_0|^2$

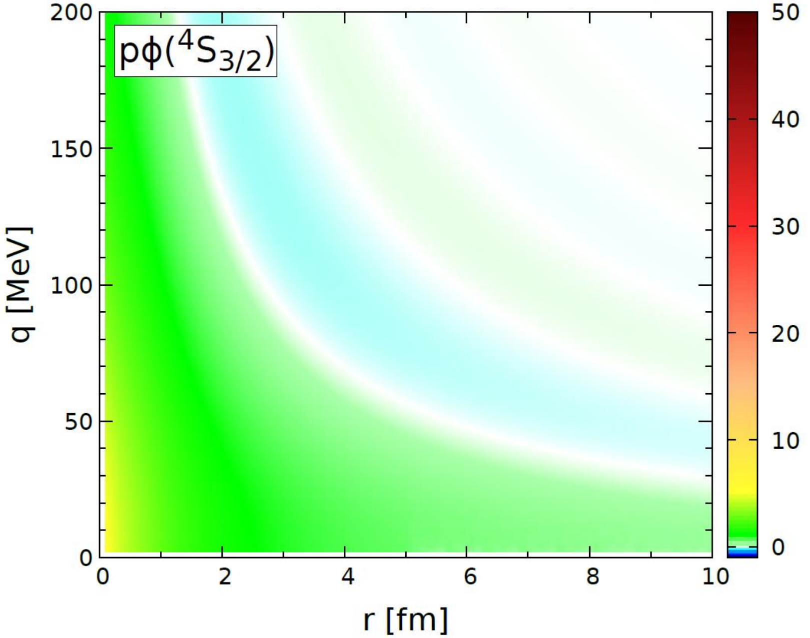

Enhancement at small *qr*
due to attraction

$^2S_{1/2}$ Channel

Parametrized potential

E. Chizzali *et al.*, PLB **848**, 138358 (2023)

Channel-couplings are neglected for simplicity

$$V^{(1/2)}(r) = \beta\left[a_1 e^{-(r/b_1)^2} + a_2 e^{-(r/b_2)^2}\right] + a_3 m_\pi^4 f(r;b_3)\frac{e^{-2m_\pi r}}{r^2}$$

Short-range interaction (first term) + TPE (second term)

Only one adjustable parameter β

default: $\beta = 7$

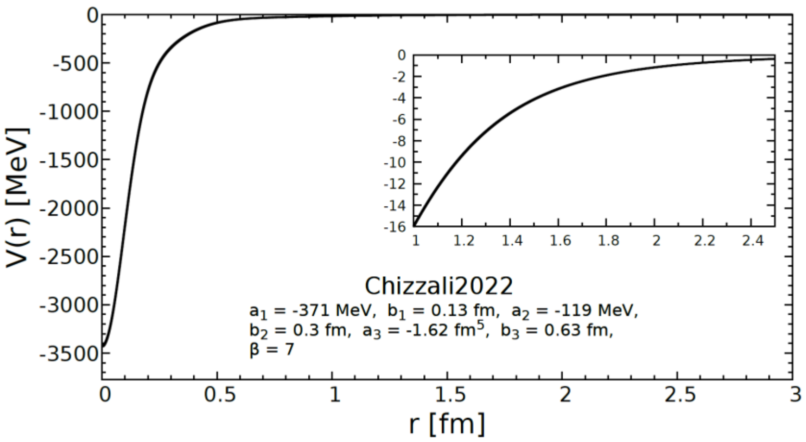

$a_0 = 1.99$ fm

$r_{\text{eff}} = 0.46$ fm

A bound state

WF change: $|\varphi_0|^2 - |j_0|^2$

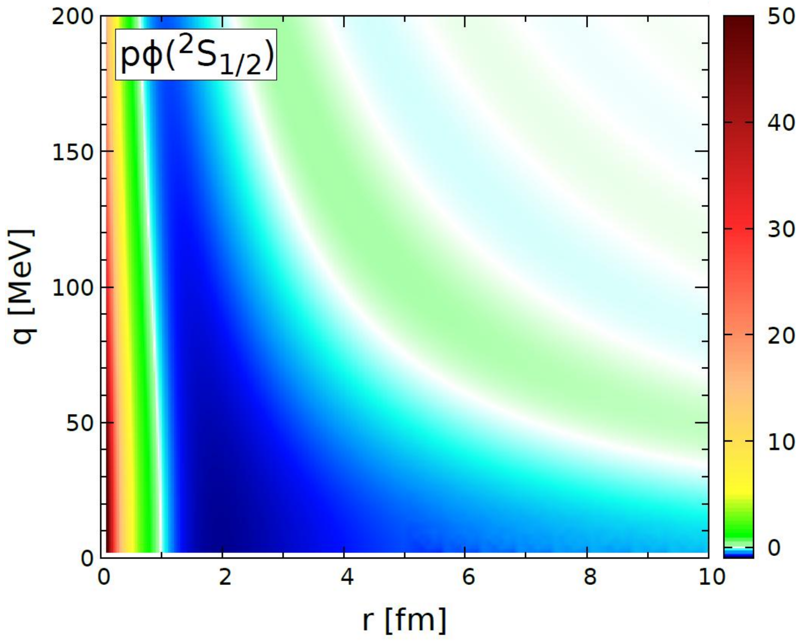

- **Strong enhancement at small qr**
- **"Negative valley" around a_0**

Dynamical Core–Corona Initialization model (DCCI)

Y. Kanakubo, Y. Tachibana, and T. Hirano, PRC **105**, 024905 (2022)

A cutting-edge dynamical model based on core–corona picture

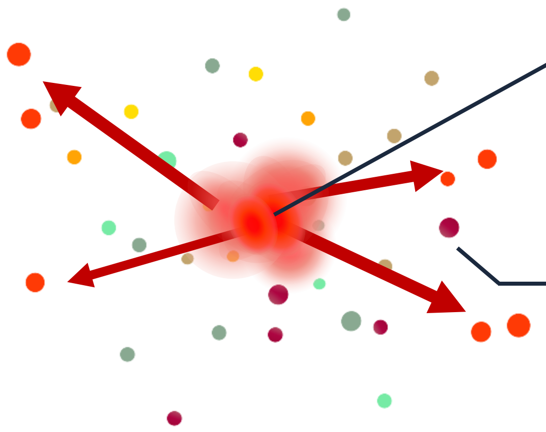

Core:
Equilibrated matter ~ QGP

Corona:
Non-equilibrium partons

Applicable to high-mult. p+p collisions

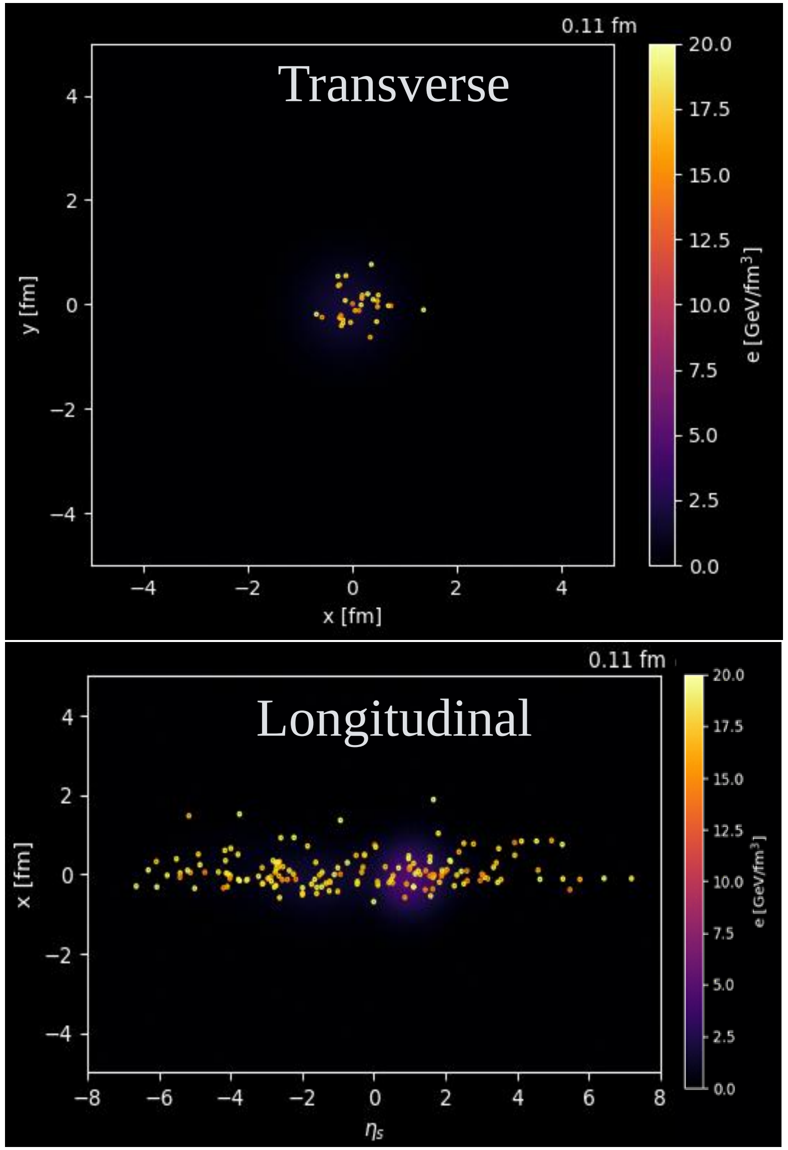

High-mult. p+p collisions at $\sqrt{s}$ = 7 TeV
Movies provided by Y. Kanakubo

DCCI2 Framework

Y. Kanakubo, Y. Tachibana, and T. Hirano, PRC **105**, 024905 (2022)

Describe the entire evolution of nuclear collision reactions

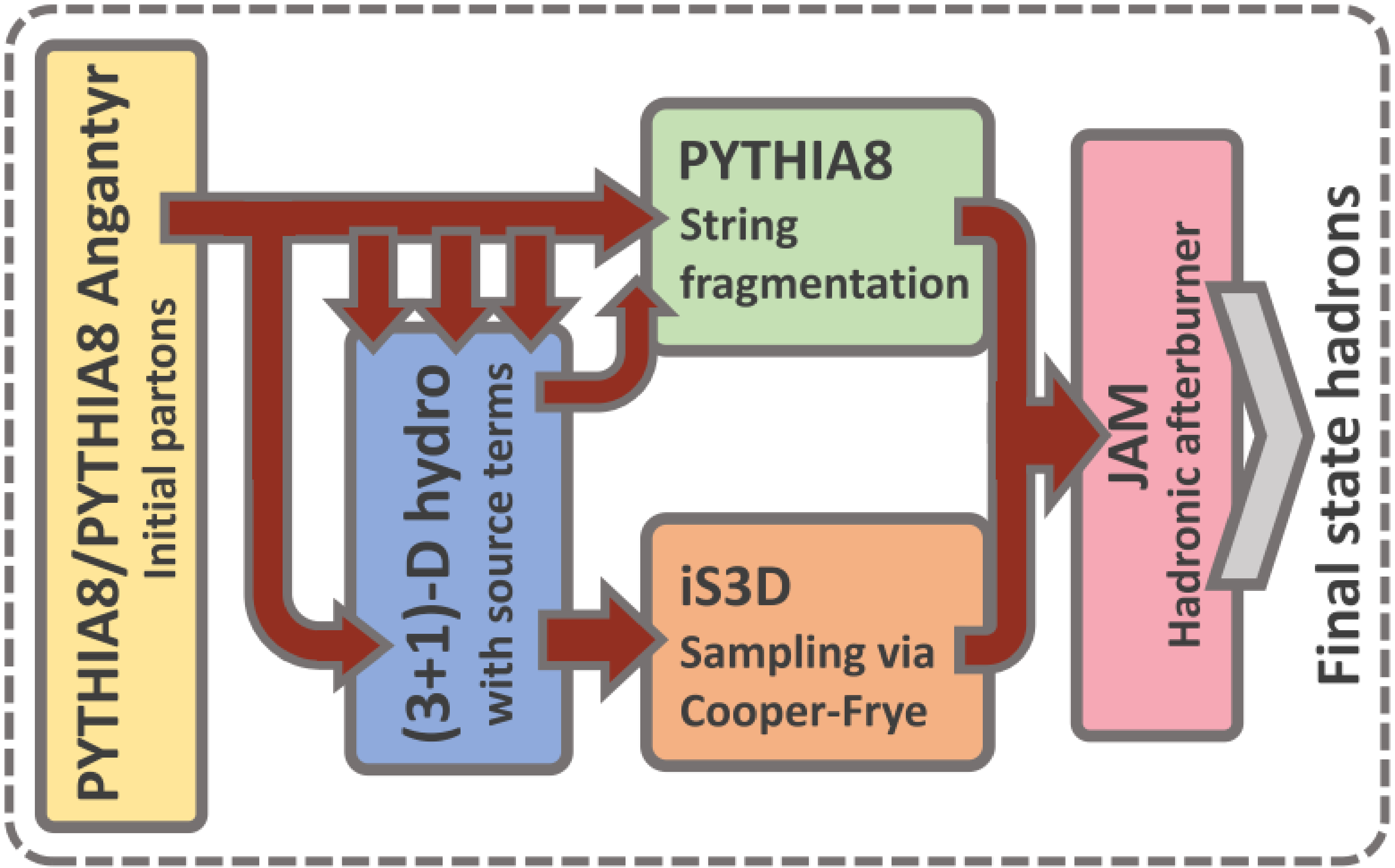

Source function that reflects realistic collision dynamics

Source Function

High-multiplicity 0-0.17% p+p collisions at $\sqrt{s} = 13$ TeV

Plot: **DCCI2 SF**, Line: Gaussian SF $S(r) \propto \exp(-r^2/4r_0^2)$ w/ $r_0 = 1.08$ fm

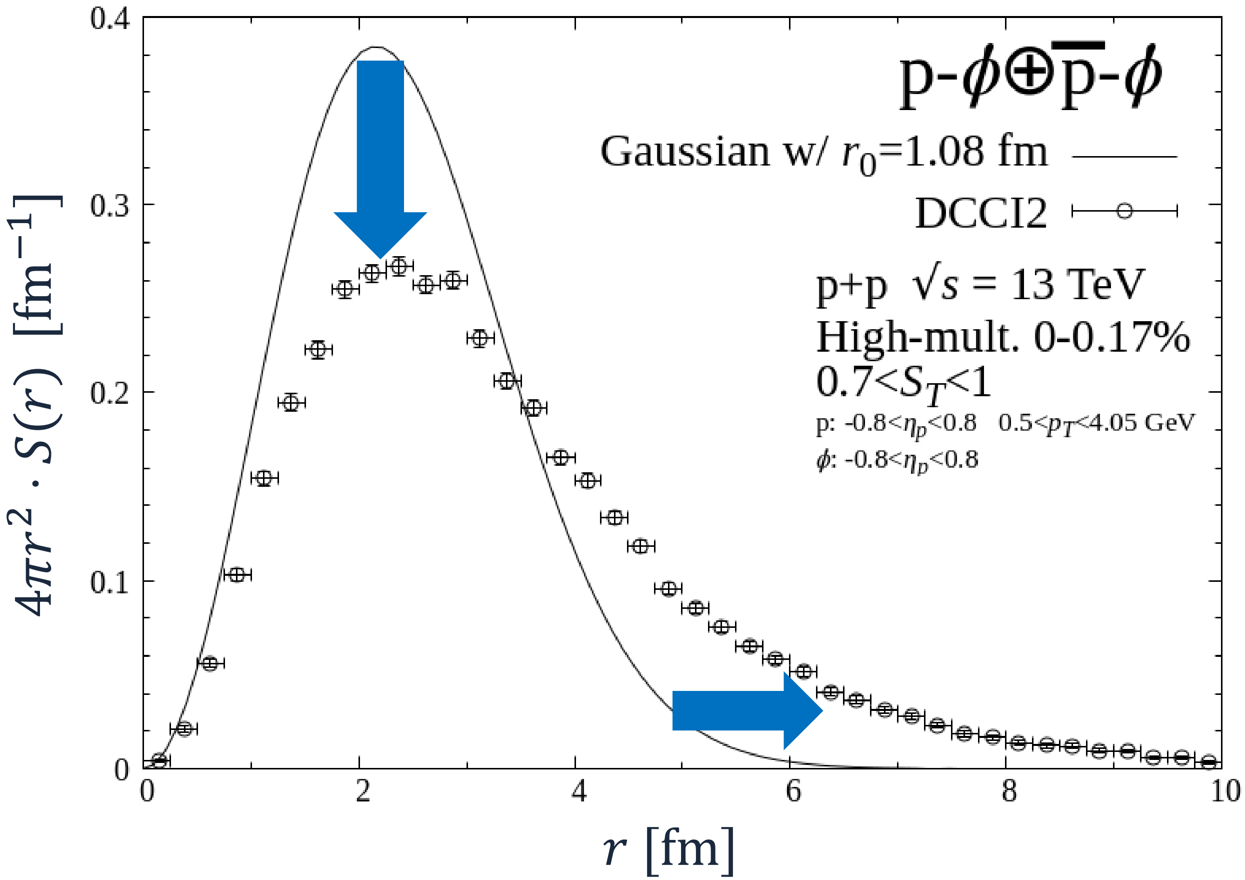

Non-Gaussian long-tail

→ Larger source size $\langle r^2 \rangle$

Mainly due to p rescatterings with surrounding pion gas "**Pion wind**"

Hadronic rescatterings even in p+p collisions

Correlation Function

Green: $C^{(3/2)}$, Blue: $C^{(1/2)}$, Red: $C^{\mathrm{tot}} = \frac{2}{3}C^{(3/2)} + \frac{1}{3}C^{(1/2)}$

Plots: **DCCI2 SF**, Lines: Gaussian SF w/ $r_0 = 1.08$ fm

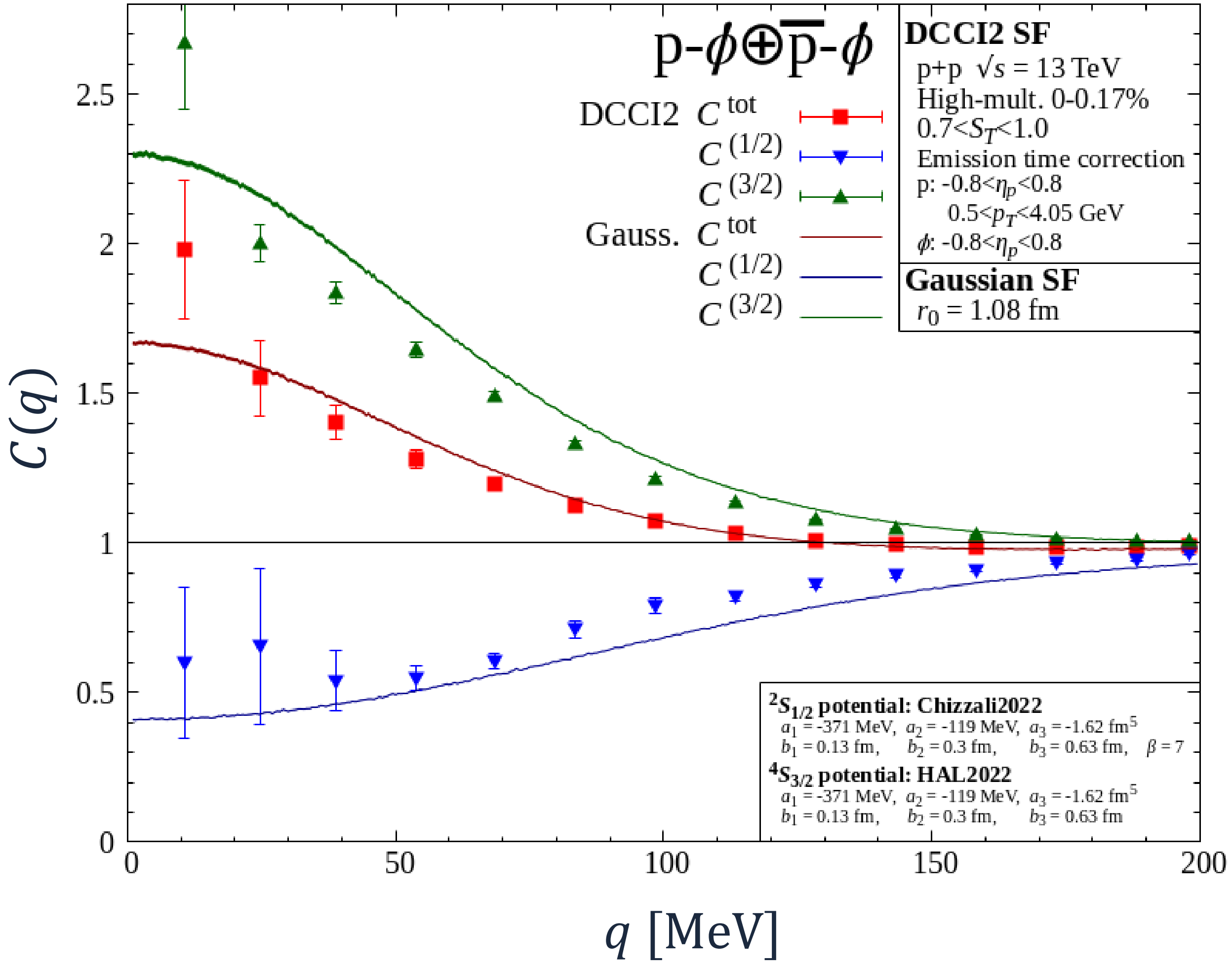

DCCI2 vs. Gaussian

- **Slightly weaker correlation**
  Due to non-Gaussian long-tail
- **Non-trivial behavior at small q**

A small but statistically significant difference

Effects of Collectivity

SF generally depends on q due to e.g., collectivity

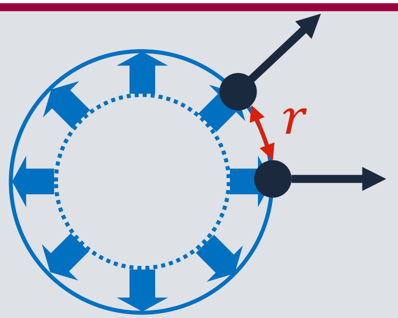

Close in position space
⇕
Close in momentum space

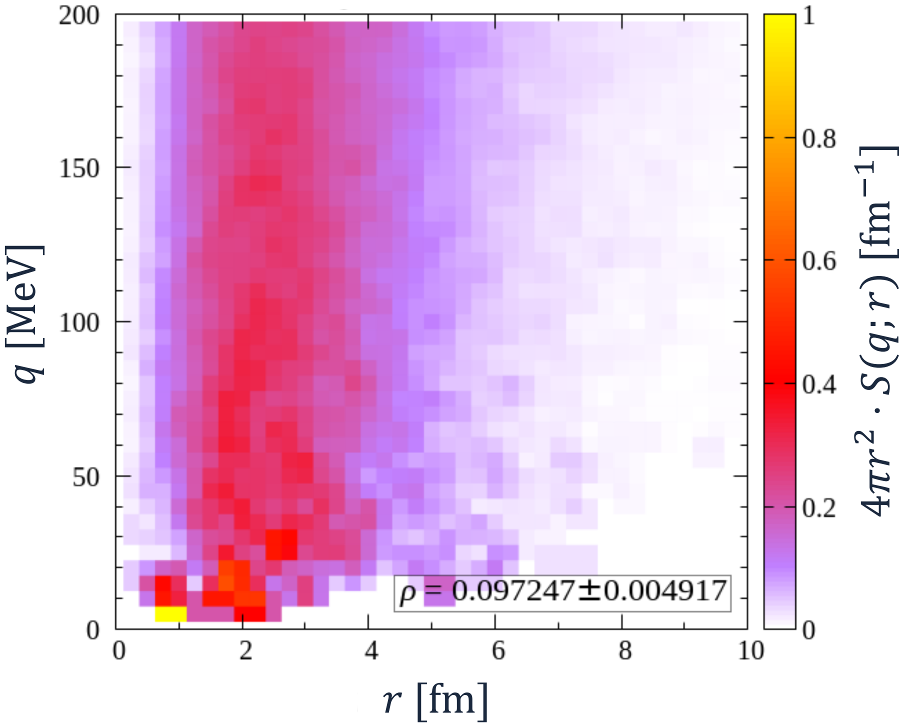

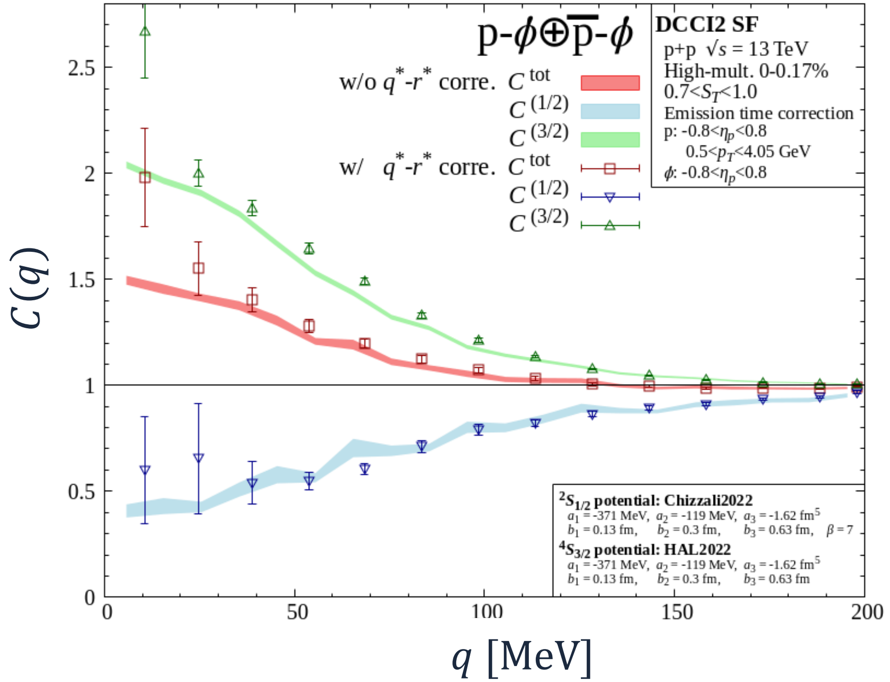

<u>Plots:</u>
W/ q–r correlation

<u>Bands:</u>
W/o q–r correlation

- Slightly positive q–r correlation
- Significant small source at small q

⇨ **CF at small q is sensitive to the WF in the scattering region**

Effects of Hadronic Afterburner

Primordial core

Direct p and ϕ from core at **hypersurface**

+ Decay → **Core w/ decay**

+ Decay + **Rescatterings** + Corona → **Full** (Comparable w/ exp. data)

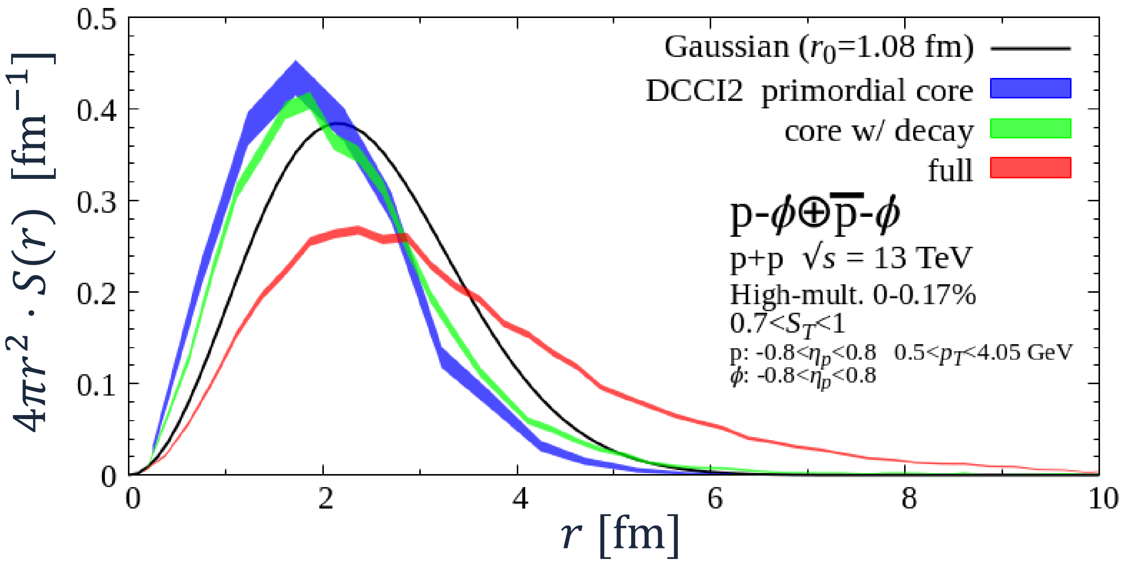

- Distribution at hypersurface ~ Gaussian
- Resonance decay → **A little long-tail**
- Hadronic rescatterings
  → **Long-tail and larger source size**

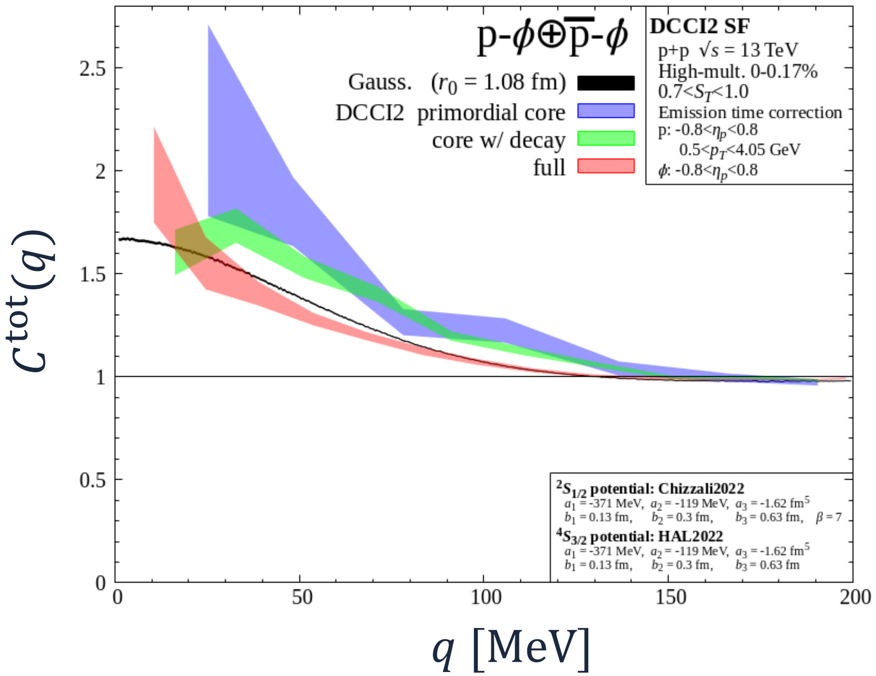

Larger effects of hadronic rescatterings than resonance decay on SF & CF

Emission Time Correction (ETC)

<u>Problem</u>

Dynamical model → **Emission time difference:** $S(\boldsymbol{q}; r^0 \neq 0, \boldsymbol{r})$

Free propagation until the other's emission

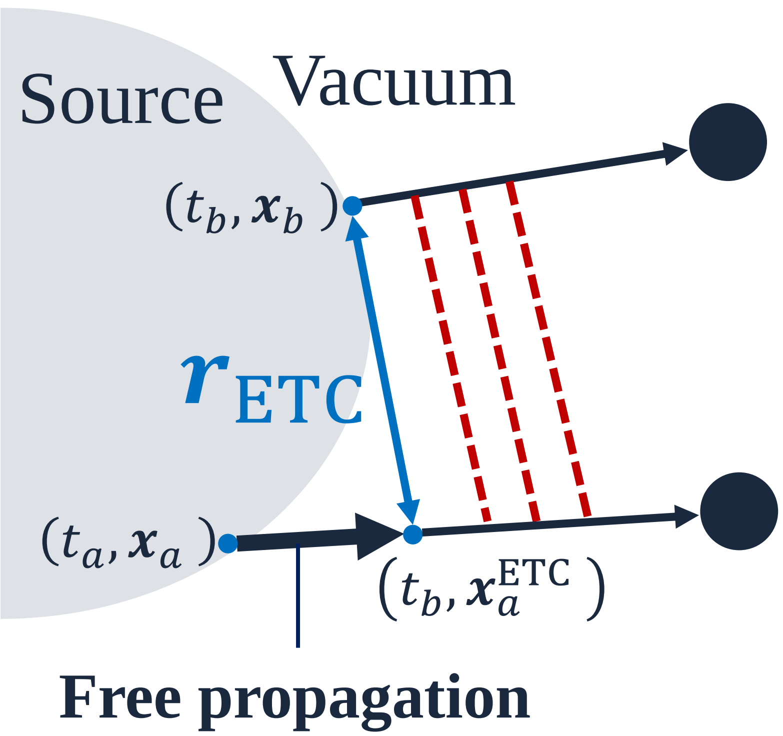

$$S(\boldsymbol{q}; r^0 \neq 0, \boldsymbol{r}) \xrightarrow{\text{ETC}} S^{\mathrm{ETC}}(\boldsymbol{q}; \boldsymbol{r}_{\mathrm{ETC}})\delta(r^0)$$

$$\boldsymbol{r}_{\mathrm{ETC}} = \boldsymbol{r} + \frac{\boldsymbol{p}_a}{E_a}(t_b - t_a)\theta(t_b - t_a) - \frac{\boldsymbol{p}_b}{E_b}(t_a - t_b)\theta(t_a - t_b)$$

Correction

Effects of Dynamical Hadron Emission

Plots: w/ ETC, Bands: w/o ETC

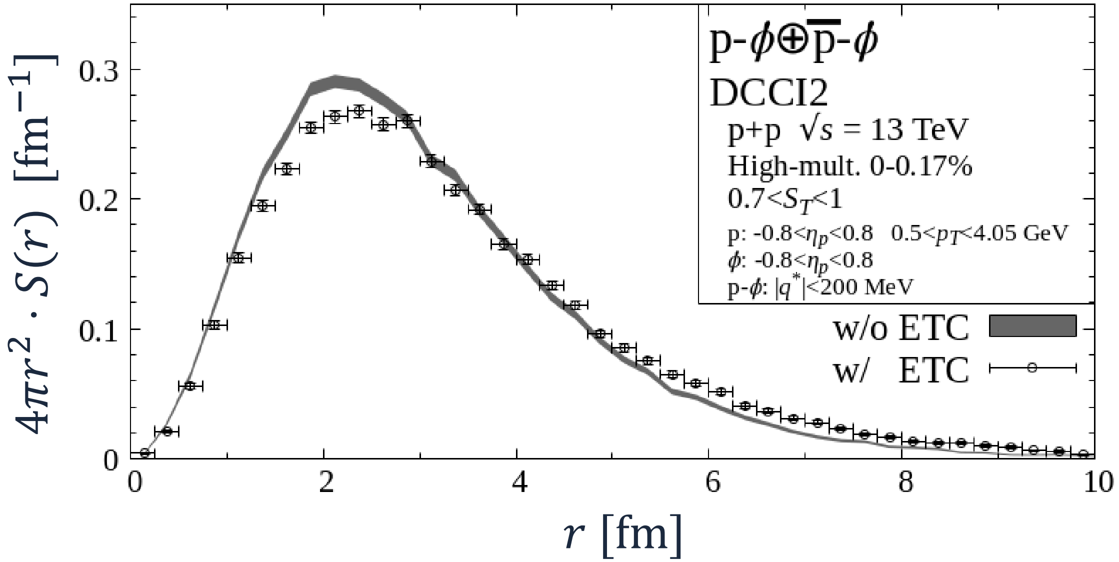

ETC slightly enlarges source size

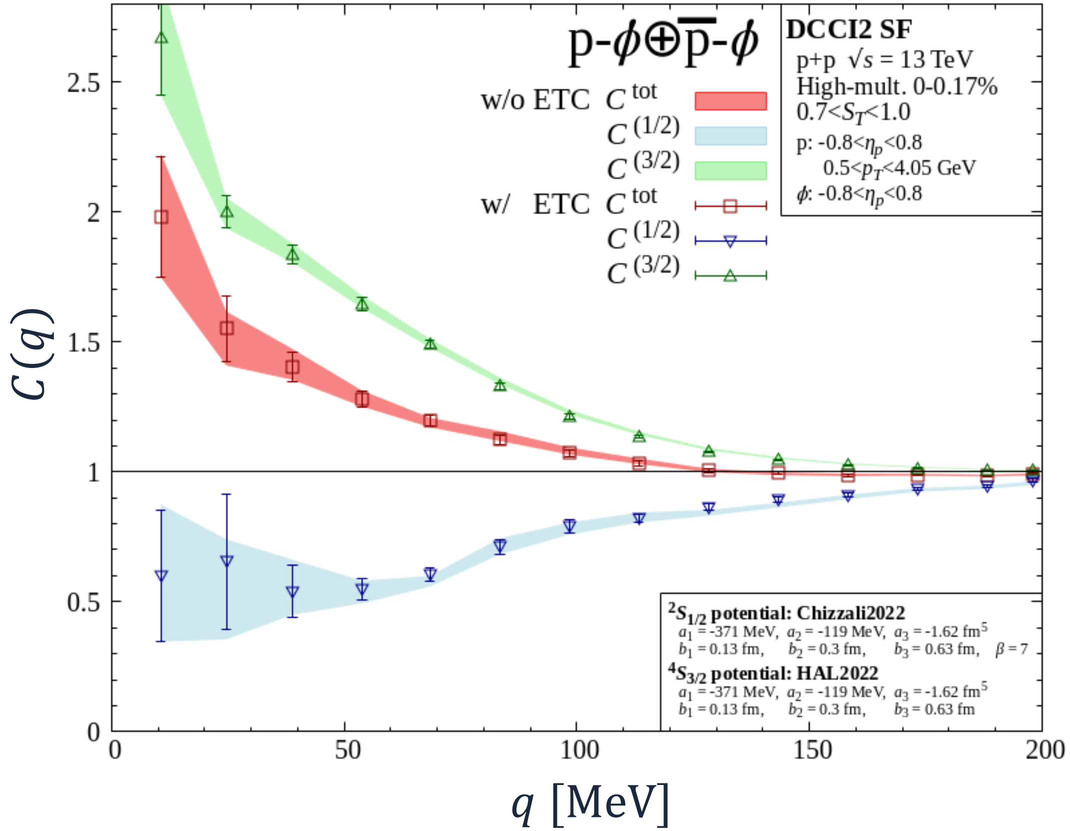

No statistically significant effects on CF in this particular case

Compare with ALICE Data

$C^{(3/2)}$: Fixed, $C^{(1/2)}$: Change with β

Compare $C^{\text{tot}} = \frac{2}{3}C^{(3/2)} + \frac{1}{3}C^{(1/2)}$ with ALICE data

$\boldsymbol{\beta = 6}$

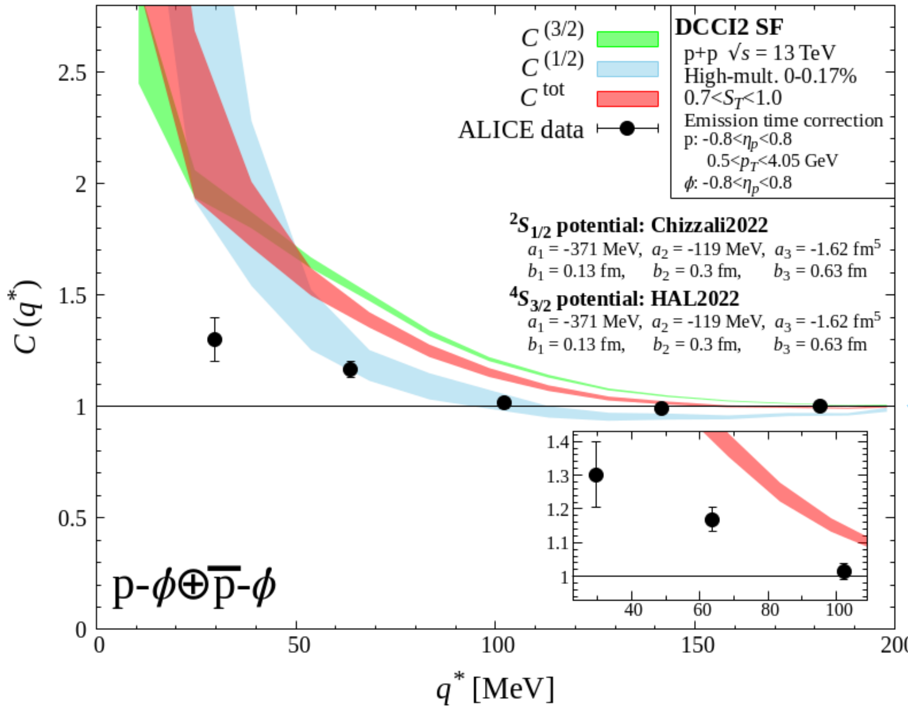

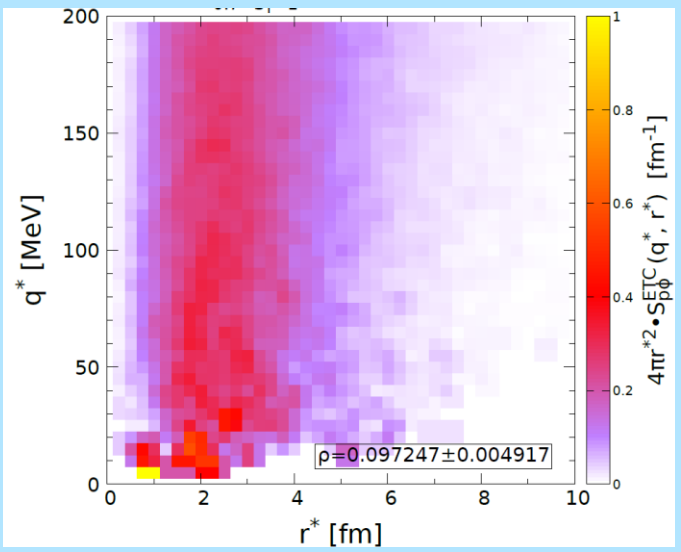

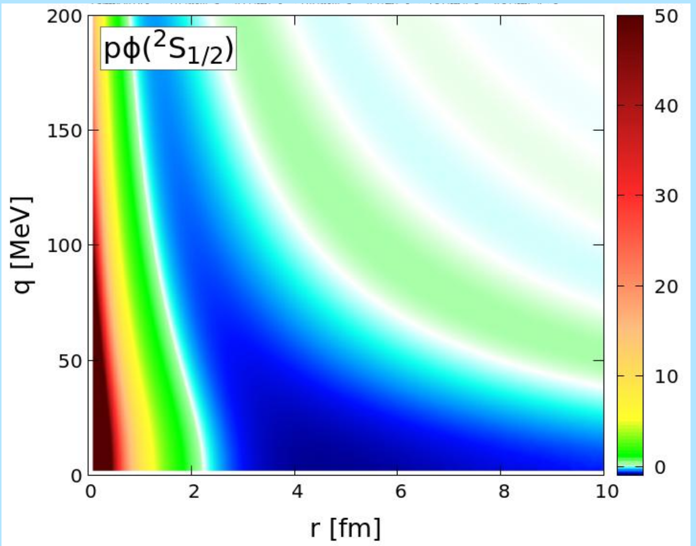

SF picks up strong positive region of WF

$C^{\text{tot}} > C^{\text{exp}}$

Compare with ALICE Data

$C^{(3/2)}$: Fixed, $C^{(1/2)}$: Change with β

Compare $C^{\text{tot}} = \frac{2}{3} C^{(3/2)} + \frac{1}{3} C^{(1/2)}$ with ALICE data

$\beta = 7$

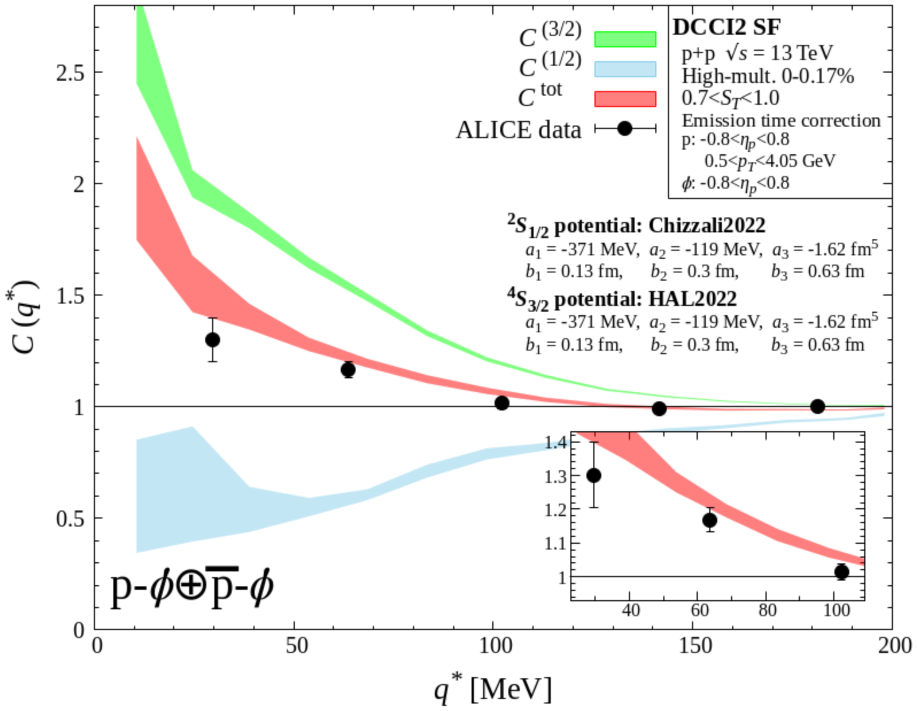

$\beta = 8$

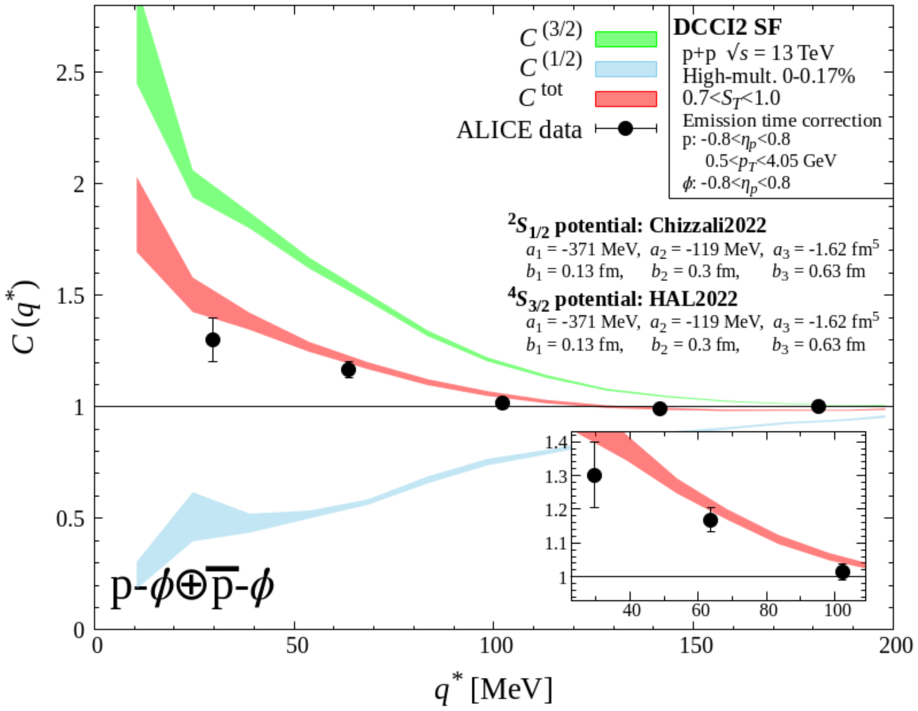

$C^{\text{tot}} \approx C^{\text{exp}}$

Compare with ALICE Data

$C^{(3/2)}$: Fixed, $C^{(1/2)}$: Change with β

Compare $C^{\text{tot}} = \frac{2}{3}C^{(3/2)} + \frac{1}{3}C^{(1/2)}$ with ALICE data

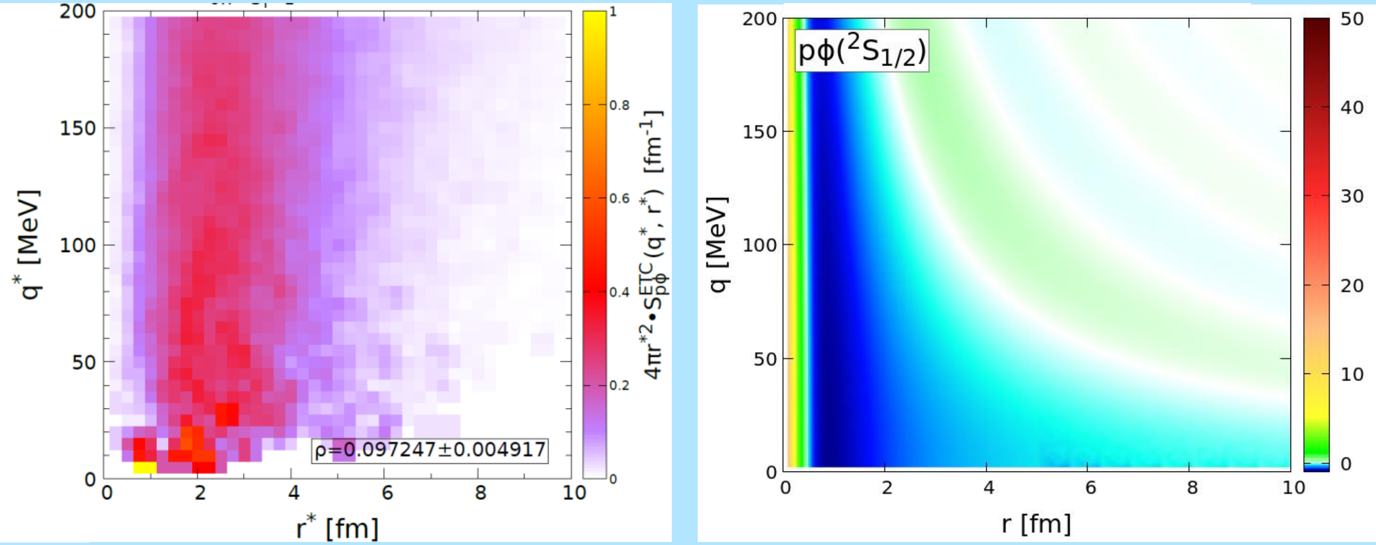

SF cannot pick up negative valley efficiently

$\boldsymbol{\beta = 9}$

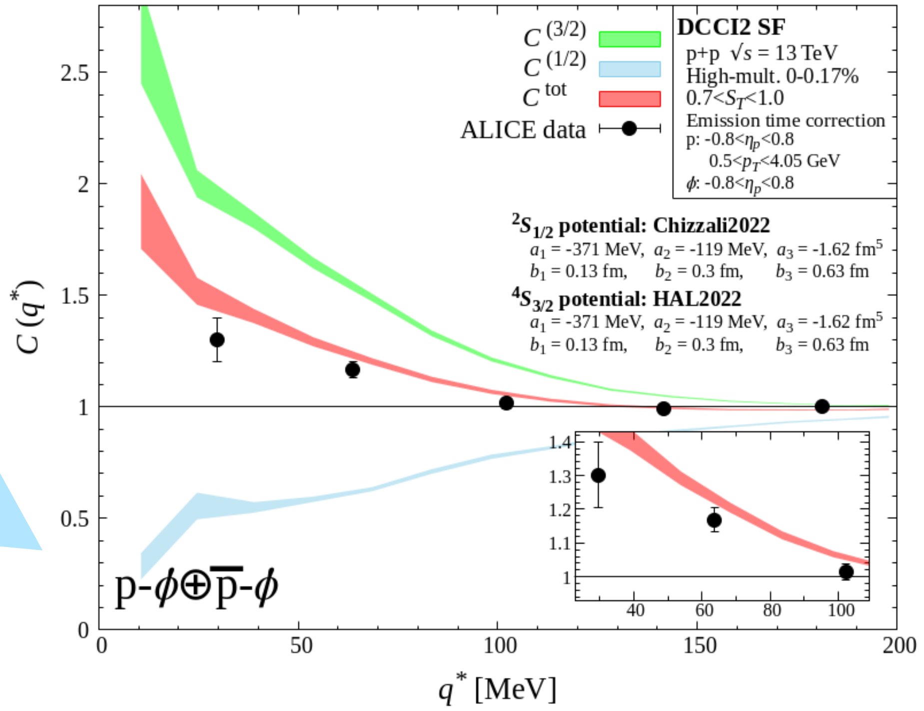

$C^{\text{tot}} > C^{\text{exp}}$

Compare with ALICE Data

$C^{(3/2)}$: Fixed, $C^{(1/2)}$: Change with β

Compare $C^{\text{tot}} = \frac{2}{3} C^{(3/2)} + \frac{1}{3} C^{(1/2)}$ with ALICE data

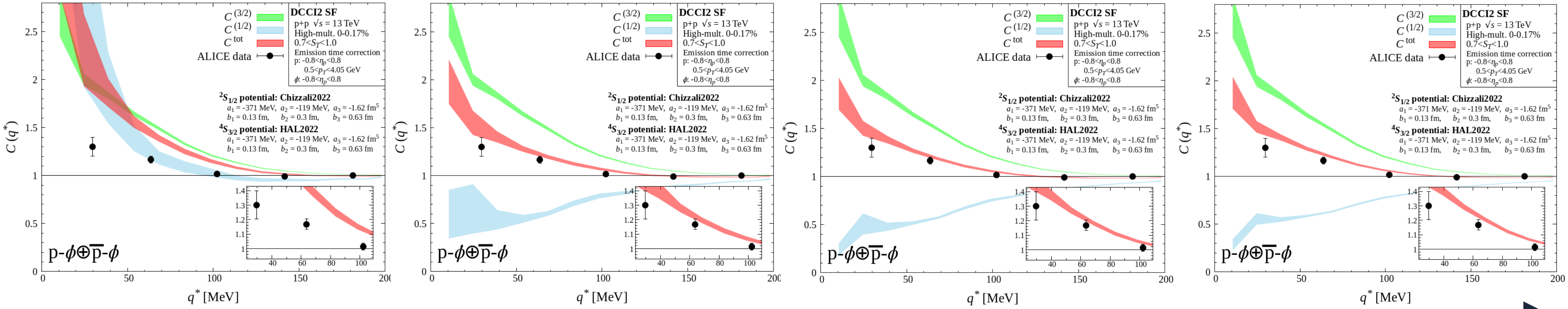

$\beta = 6$	$\beta = 7$	$\beta = 8$	$\beta = 9$
$a_0 = 4.54$ fm	$a_0 = 1.99$ fm	$a_0 = 1.23$ fm	$a_0 = 0.85$ fm
$E_B = 2.3$ MeV	$E_B = 13.3$ MeV	$E_B = 37.5$ MeV	$E_B = 93.1$ MeV

Overestimate — Agree within errors — Overestimate

Summary

pϕ femtoscopy using SF from a dynamical model (DCCI2)

Effects of Collision Dynamics

Small but statistically significant

- ✓ SF has non-Gaussian tail mainly due to **hadronic rescatterings**
- ✓ SF depends on relative momentum due to e.g., **collectivity**

Phenomenological Constraint on Interaction

- ✓ Indication of a bound state in ${}^2S_{1/2}$ channel ($E_B \cong 10$–70 MeV)

  Slightly different but qualitatively consistent with that using Gaussian SF

Importance of using SF that reflects collision dynamics

for precise studies of hadron interactions via femtoscopy

Backup

Core–Corona Ratio

Y. Kanakubo, Y. Tachibana, and T. Hirano, PRC **105**, 024905 (2022)

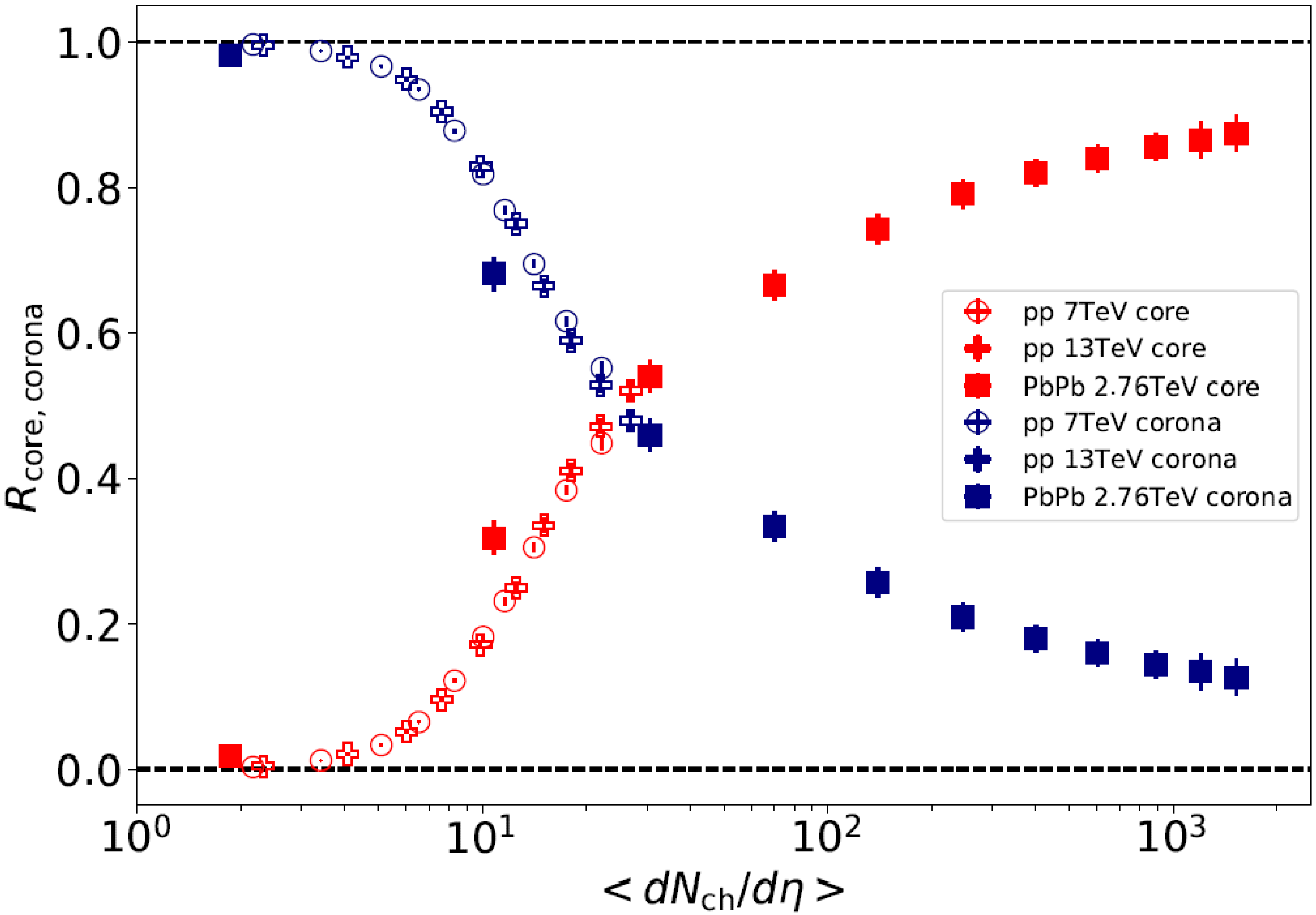

According to DCCI2

$R_{\mathbf{core}} \sim 0.5$

in high-multiplicity p+p collisions at $\sqrt{s} = 13$ TeV

Koonin-Pratt Formula S. E. Koonin, PLB **70**, 43 (1977); S. Pratt, PRL **53**, 1219 (1984)

Assumptions

- **Chaotic source** ~ thermal equilibrium
- **Closed system after emission** ~ in vacuum propagation
- (Same time approximation)
- On-shell approximation

$$C(\boldsymbol{q},\boldsymbol{P}) = \frac{\int d^4x_a d^4x_b\, S_a(\boldsymbol{p}_a; x_a) S_b(\boldsymbol{p}_b; x_b) |\varphi(\boldsymbol{q};\boldsymbol{r})|^2}{\int d^4x_a\, S_a(\boldsymbol{p}_a; x_a) \int d^4x_b\, S_b(\boldsymbol{p}_b; x_b)}$$

Pair Rest Frame ($\boldsymbol{P} = \mathbf{0}$)

Integrate out CM

$$C(\boldsymbol{q}) = \int d^3r\; S(\boldsymbol{q};\boldsymbol{r})\; |\varphi(\boldsymbol{q};\boldsymbol{r})|^2$$

Lednický-Lyuboshits Model

R. Lednický and V. L. Lyuboshits, Yad. Fiz. **35**, 1316 (1981)

$$C(q) = 1 + \int_0^\infty dr 4\pi r^2 S(q;r)\left[|\varphi_0(q;r)|^2 - |j_0(qr)|^2\right]$$

<u>Assumptions</u>

- **Gaussian SF**: $S(q;r) \approx S(r) \propto \exp\left(-\frac{r^2}{4r_0^2}\right)$
- **Asymptotic WF** (+ effective range correction)

$$C(q) = 1 + \frac{|f_0(q)|^2}{2r_0^2} F_3\left(\frac{r_{\mathrm{eff}}}{r_0}\right) + \frac{2\mathrm{Re} f_0(q)}{\sqrt{\pi} r_0} F_1(2qr_0) - \frac{\mathrm{Im} f_0(q)}{r_0} F_2(2qr_0)$$

$F_1, \ldots, F_3$: Known functions, $f_0(q) = \frac{1}{q\cot\delta_0(q) - iq} \approx \frac{1}{-\frac{1}{a_0} + \frac{1}{2} r_{\mathrm{eff}} q^2 - iq}$

CF becomes a function of a_0, r_{eff}, and r_0

WF Change: Interaction-Dependence

Weak **Attractive potential w/ a bound state** Strong

$\boldsymbol{\beta = 6}$	$\boldsymbol{\beta = 7}$	$\boldsymbol{\beta = 8}$	$\boldsymbol{\beta = 9}$
$a_0 = 4.54$ fm	$a_0 = 1.99$ fm	$a_0 = 1.23$ fm	$a_0 = 0.85$ fm
$E_B = 2.3$ MeV	$E_B = 13.3$ MeV	$E_B = 37.5$ MeV	$E_B = 93.1$ MeV

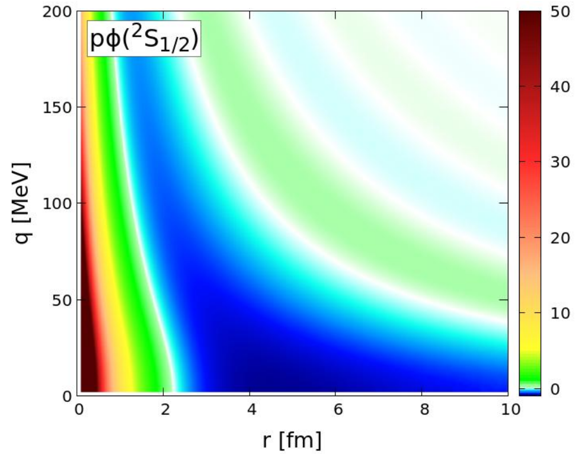

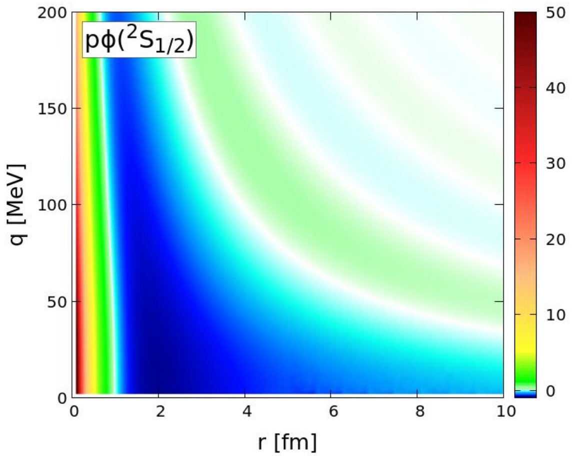

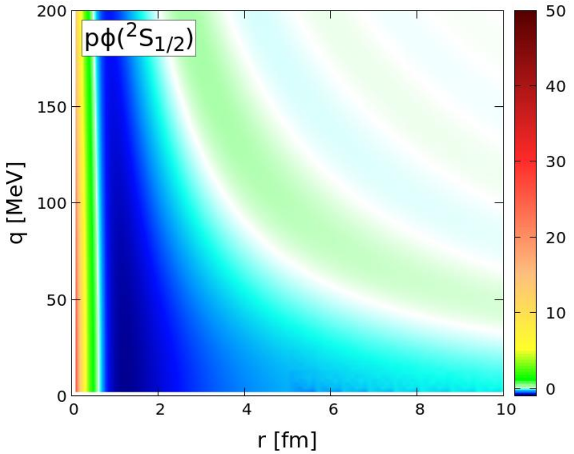

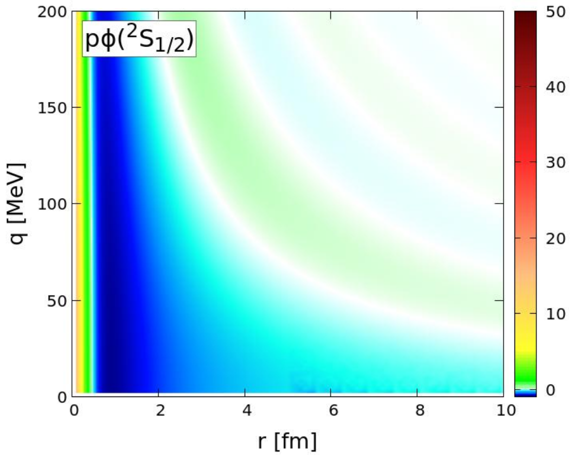

The negative valley moves towards the small r region